Geometric preservation of 2D digital objects under rigid motions

Phuc Ngo, Nicolas Passat, Yukiko Kenmochi, Isabelle Debled-Rennesson

Noname manuscript No.
(will be inserted by the editor)

Geometric preservation of 2D digital objects under rigid motions

Phuc Ngo · Nicolas Passat · Yukiko Kenmochi · Isabelle Debled-Rennesson

Received: date / Accepted: date

Abstract Rigid motions (*i.e.* transformations based on translations and rotations) are simple, yet important, transformations in image processing. In Euclidean spaces, namely $\mathbb{R}^n$, they are both topology and geometry preserving. Unfortunately, these properties are generally lost in $\mathbb{Z}^n$. In particular, when applying a rigid motion on a digital object, one generally alters its structure but also the global shape of its boundary. These alterations are mainly caused by (re)digitization during the transformation process. In this specific context of digitization, some solutions for the handling of topological issues were proposed in $\mathbb{Z}^2$ and/or $\mathbb{Z}^3$. In this article, we also focus on geometric issues, in the case of $\mathbb{Z}^2$. More precisely, we propose a rigid motion algorithmic scheme that relies on an initial polygonization and a final digitization step. The intermediate modeling of a digital object of $\mathbb{Z}^2$ as a piecewise affine object of $\mathbb{R}^2$ allows us to avoid the geometric alterations generally induced by standard pointwise rigid motions. The crucial step is then related to the final (re)digitization of the polygon back to $\mathbb{Z}^2$. To tackle this issue, we propose a new notion of quasi-regularity that provides sufficient conditions to be fulfilled by an object for guaranteeing both topology and geometry preservation, in particular the preservation of the convex/concave parts of its boundary.

Keywords Rigid motions · Geometry and topology preservation · Polygonization · (Re)digitization · Quasi-r-regularity

P. Ngo (corresponding author)
Université de Lorraine, CNRS, LORIA, France
Tel: (+33) 03.83.59.84.30
Fax : (+33) x xx xx xx xx
E-mail: hoai-diem-phuc.ngo@loria.fr

N. Passat
Université de Reims Champagne-Ardenne, CReSTIC, France
E-mail: nicolas.passat@univ-reims.fr

Y. Kenmochi
Université Paris-Est, CNRS, LIGM, France
E-mail: yukiko.kenmochi@esiee.fr

I. Debled-Rennesson
Université de Lorraine, CNRS, LORIA, France
E-mail: isabelle.debled-rennesson@loria.fr

1 Introduction

Image processing and computer vision applications often require to manipulate discrete models of images. Among the various existing discrete models (*e.g.* meshes, point clouds), digital images, defined as finite sets of points on $\mathbb{Z}^n$, are of wide importance. Indeed, digital images naturally fit with most image acquisition devices based on a Cartesian sampling of the observed scene (*e.g.* medical imaging scanners, remote sensing optical imagers). Being able to manipulate digital objects defined as finite subsets of $\mathbb{Z}^n$ is then of paramount importance.

Such manipulations can involve rigid or non-rigid transformations. Non-rigid transformations are generally devoted to emphasize the correspondence between different scenes (*e.g.* for registration [1]) or to fit a given model onto a structure of interest (*e.g.* for segmentation [2]). In this context, topological preservation is crucial while geometry is devoted to evolve. Rigid transformations are much simpler operations. They are basically involved in the handling of digital objects, or preprocessing tasks. In this context, both topology and geometry preservation are crucial. Indeed, the structure of the digital objects has to be preserved, but their shape should also remain unchanged.

In this article, we are interested in rigid transformations on digital objects. More precisely, we focus on rigid motions. Rigid motions are defined as compositions of translations and rotations, namely the two most fundamental operations for "moving" objects in a scene. Intuitively, such rigid motions have to preserve the object; this is indeed the case in our Euclidean world. In $\mathbb{R}^n$, rigid motions are bijective, isometric operations; the structure of the handled objects is preserved such as their geometrical properties, and in particular their shape.

This is no longer true in the Eulerian space. This is mainly due to the sparse structure of $\mathbb{Z}^n$, that implies a non-continuous behaviour of rigid motions [3]. In other words, when applying a rigid motion operator $\mathcal{T}$ on a digital point $\mathsf{p} \in \mathbb{Z}^n$, the resulting value $\mathcal{T}(\mathsf{p})$ generally lies out of $\mathbb{Z}^n$. It is then necessary to find a way for carrying $\mathcal{T}(\mathsf{p})$ back to the Cartesian grid. The induced approximation may lead to altering the topological structure of the object X containing p. It may also modify the global shape of X by slightly moving its different points in a heterogeneous way [4].

In the case of $\mathbb{Z}^2$, some strategies were recently investigated for providing topological guarantees when applying a rigid motion on digital objects [5,6]. However, such approaches do not provide geometric guarantees. This weakness is mainly due to the fact that rigid motions are carried out in a pointwise way: each point p of X is transformed independently from the others, thus forbidding a coherent handling of the global shape of the object.

Our proposed solution for tackling the issue of geometry preservation is to consider an intermediate, continuous, representation $P(\mathsf{X})$ of the object X of $\mathbb{Z}^2$. More precisely, we propose to define $P(\mathsf{X})$ as a polygon modeling the general shape of the digital boundary of X. Such a polygon, as a piecewise affine object of $\mathbb{R}^2$, can be processed in a topology and geometry preserving way by the transformation $\mathcal{T}$. The main issue remaining to be tackled is then related to the (re)digitization of the polygon $\mathcal{T}(P(\mathsf{X}))$ back to $\mathbb{Z}^2$. Such digitization problem is related to pioneering works [7] developed by Pavlidis in the 80's. However, while Pavlidis was interested in the digitization of "smooth" objects, *i.e.* objects of $\mathbb{R}^2$ with boundaries having differentiable properties, we have to consider here some polygons, with non-differentiable boundary points.

This article is an extended and improved version of the conference paper [8]. A first contribution, in Sec. 3, is a sufficient condition for guaranteeing the preservation of connectedness during the process of digitization of an object of $\mathbb{R}^2$. This condition, defined under the name of *quasi-r-regularity*, can be seen as an analogue of the *r-regularity* proposed by Pavlidis for smooth objects [7]. This condition is then involved in the next two sections, for preserving satisfactory geometry and topology properties during the rigid motion of a digital object. In Sec. 4, we describe our rigid motion process in the case where the input digital object is well-composed and convex. (In such case, the induced polygon is also convex.) The transformed object will have its topology unchanged and will remain convex. In Sec. 5, we consider, more generally, the case of well-composed objects, non-necessarily convex. We also show that under the conditions of quasi-r-regularity, the transformed object remains well-composed and preserves the global geometry of its shape. Sec. 6 provides some experimental results of the proposed framework for rigid motions on convex and non-convex digital objects. A concluding discussion is proposed in Sec. 7. In order to make this work self-contained, we recall, in Sec. 2, some basic definitions and notations related to rigid motions, and the various notions of regularity on digital images.

2 Rigid motions and digitization

2.1 Rigid motions on $\mathbb{R}^2$

A rigid motion $\mathcal{T}$ in the Euclidean space $\mathbb{R}^2$ is defined, for any point $\mathbf{x} = (x, y)^t$ as

$$\mathcal{T}(\mathbf{x}) = \begin{pmatrix} \cos\theta & -\sin\theta \\ \sin\theta & \cos\theta \end{pmatrix} \begin{pmatrix} x \\ y \end{pmatrix} + \begin{pmatrix} a \\ b \end{pmatrix} \qquad (1)$$

where $\theta \in [0, 2\pi)$ is a rotation angle, and $(a, b)^t \in \mathbb{R}^2$ is a translation vector.

Let X be a continuous object in the Euclidean space $\mathbb{R}^2$. (In the sequel, we will implicitly consider that X is finite and connected.) The transformation $\mathcal{T}$ is bijective, isometric and orientation-preserving. Then, the transformed object $\mathcal{T}(\mathrm{X})$ has the same shape, *i.e.* the same geometry and topology, as X. In the next subsections, we will observe that these properties are generally lost during the digitization process required to define rigid motions on $\mathbb{Z}^2$ from rigid motions on $\mathbb{R}^2$.

2.2 Digitization and topology preservation

A digital object $\mathsf{X} \subset \mathbb{Z}^2$ is generally the result of a digitization process applied on a continuous object $\mathrm{X} \subset \mathbb{R}^2$. We consider the Gauss digitization [9], which is simply the intersection of a continuous object X with the Cartesian grid $\mathbb{Z}^2$

$$\mathsf{X} = \mathrm{X} \cap \mathbb{Z}^2 \qquad (2)$$

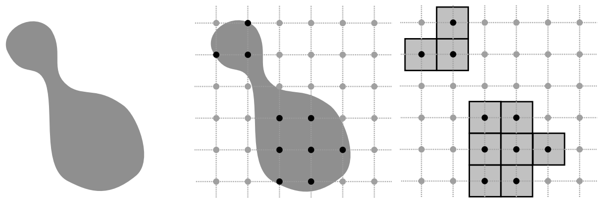

Fig. 1 (a) A continuous object X in $\mathbb{R}^2$. (b) A Gauss digitization of X, leading to the definition of X which is composed by the black points of $\mathbb{Z}^2$ within X. (c) The digital object X represented as a set of pixels, *i.e.* by associating to each point p of X the unit square corresponding to its Voronoi cell. The objects X and X are not topologically equivalent: the digitization process led to a disconnection, due to the resolution of the Cartesian grid, not sufficiently fine for catching the shape of X.

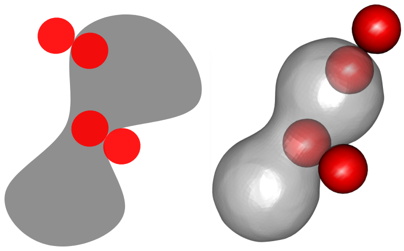

Fig. 2 r-regular objects in (a) $\mathbb{R}^2$ and (b) $\mathbb{R}^3$, in grey. Examples of couples of tangent balls of radius r, fitting the boundary of the objects, are provided in red.

The object X is a subset of $\mathbb{Z}^2$; but from an imaging point of view, it can also be seen as a subset of pixels, *i.e.* unit squares defined as the Voronoi cells of the points of X within $\mathbb{Z}^2$. Based on these different models, the structure of X can be defined in various topological frameworks which are mainly equivalent [10] to that of digital topology [11]. However, this digital topology of X is often non-coherent with the continuous topology of X. This fact is illustrated in Fig. 1, where a connected continuous object X leads, after Gauss digitization, to a disconnected digital object X.

In the literature, various studies proposed conditions for guaranteeing the preservation of topology of digitized objects [12–14]. In particular, in [7] Pavlidis introduced the notion of *r-regularity*.

Definition 1 **(r-regularity [7])** An object $X \subset \mathbb{R}^n$, $n = 2, 3$, is *r-regular* if for each boundary point of X, there exist two tangent open balls of radius r, lying entirely in X and its complement $\overline{X}$, respectively.

Illustrations of r-regularity for $n = 2, 3$ are given in Fig. 2. The notion of r-regularity is based on classical concepts of differential geometry. In particular, r-regularity is strongly related to bounded values of curvatures, parametrized by the resolution of the digitization sampling. Pavlidis proved the homeomorphic equivalence of an r-regular continuous, smooth, object X and its digital counterpart X, for a sufficiently dense sampling.

Proposition 1 **([7])** *An r-regular object $X \subset \mathbb{R}^2$ has the same topological structure as its digitized version $\mathsf{X} = X \cap \mathbb{Z}^2$ if $r \geq \frac{\sqrt{2}}{2}$.*

In addition, it was shown that the digitization process of an r-regular object yields a well-composed object [13], whose definition relies on standard concepts of digital topology, recalled hereafter, for the sake of completeness.

Two distinct points $\mathsf{p}, \mathsf{q} \in \mathbb{Z}^2$, are k-adjacent if

$$\|\mathsf{p} - \mathsf{q}\|_\ell \leq 1 \tag{3}$$

with $k = 4$ (resp. 8) when $\ell = 1$ (resp. ∞). From the reflexive–transitive closure of the k-adjacency relation on a finite subset $\mathsf{X} \subset \mathbb{Z}^2$, we derive the k-connectivity relation on X. It is an equivalence relation, whose equivalence classes are called the k-connected components of X. Due to paradoxes related to the discrete version of the Jordan theorem [15], dual adjacencies are used for X and its complement $\overline{\mathsf{X}}$, namely $(4, 8)$- or $(8, 4)$-adjacencies [16].

The notion of well-composedness [17] has been introduced to characterize the digital objects whose structure intrinsically avoids the topological issues of the Jordan theorem.

Definition 2 **(Well-composed sets [17])** A digital object $\mathsf{X} \subset \mathbb{Z}^2$ is *well-composed* if each 8-connected component of X and of its complement $\overline{\mathsf{X}}$ is also 4-connected.

This definition implies that the boundary[1] of X is a set of 1-manifolds whenever X is well-composed (see Fig. 3). In particular, there exists a strong link between r-regularity and well-composedness.

Proposition 2 **([13])** *If an object $X \subset \mathbb{R}^2$ is r-regular, with $r \geq \frac{\sqrt{2}}{2}$, then $\mathsf{X} = X \cap \mathbb{Z}^2$ is a well-composed digital object.*

2.3 Digitized rigid motions

If we straightforwardy apply a rigid motion $\mathcal{T}$, such as defined in Eq. (1), to a digital object $\mathsf{X} \subset \mathbb{Z}^2$, we generally obtain a transformed object $\mathcal{T}(\mathsf{X}) \not\subset \mathbb{Z}^2$. In order

[1] The boundary of X is defined here as the boundary of the continuous object obtained as the union of the closed Voronoi cells associated to the points of X, in $\mathbb{R}^2$.

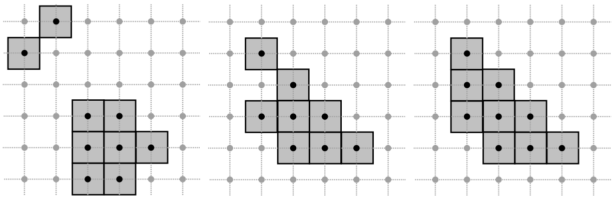

(a) (b) (c)

Fig. 3 (a) $\mathsf{X} \subset \mathbb{Z}^2$ (in grey) is neither connected, nor well-composed. (b) X is 8-connected, but neither 4-connected nor well-composed. (c) X is 4-connected and well-composed.

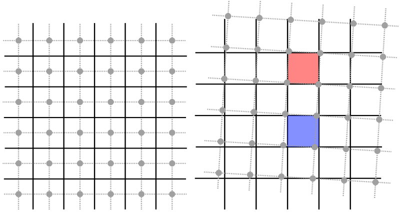

(a) (b)

Fig. 4 Examples of non-injectivity and non-surjectivity of rigid motions followed by a digitization. (a) The square grid of $\mathbb{Z}^2$ and the associated Voronoi cell boundaries. (b) Rigid motion followed by a digitization applied on the square grid of (a); the red and blue pixels correspond to non-surjectivity and non-injectivity cases, respectively.

to obtain a result in $\mathbb{Z}^2$, we further need a digitization operator

$$\mathfrak{D} : \mathbb{R}^2 \to \mathbb{Z}^2 \tag{4}$$

which can be, for instance, the standard rounding function. Then, a digital analogue of $\mathfrak{T}$ can be defined as the composition of $\mathfrak{T}$, (restricted to $\mathbb{Z}^2$) with such digitization operator, *i.e.* $\mathfrak{D} \circ \mathfrak{T}_{|\mathbb{Z}^2}$.

As stated above, rigid motions on $\mathbb{R}^2$ are bijective. By contrast, rigid motions followed by a digitization operator are, in general, neither injective nor surjective. This may lead to unwanted results, such as conflicted or empty pixels, as illustrated in Fig. 4. To overcome such issues, we generally consider the inverse of the rigid motion to define the discrete analogue of $\mathfrak{T}$ on $\mathbb{Z}^2$ by setting

$$\mathcal{T}_{Point}^{-1} = \mathfrak{D} \circ \mathfrak{T}_{|\mathbb{Z}^2}^{-1} \tag{5}$$

In other words, we use a backward model for the computation of the rigid motion of a digital object X. Indeed, we consider that the object $\mathcal{T}_{Point}(\mathsf{X}) \subset \mathbb{Z}^2$ induced by the digitized version of the rigid motion $\mathfrak{T}$ is defined such that:

$$\mathsf{p} \in \mathcal{T}_{Point}(\mathsf{X}) \Leftrightarrow \mathcal{T}_{Point}^{-1}(\mathsf{p}) \in \mathsf{X} \tag{6}$$

2.4 Topology and geometry alterations caused by digitized rigid motions

This backward model can also be interpreted, in a forward way, as the digitization of a transformed continuous object. Indeed, let us denote by $V(\mathsf{X}) \subset \mathbb{R}^2$ the continuous object obtained as the union of the closed Voronoi cells associated to the points of X; in other words, let us consider the digital object as its set of pixels. Then, the transformed digital object $\mathcal{T}_{Point}(\mathsf{X})$ is obtained as the Gauss digitization of the transformed object resulting from the rigid motion of $V(\mathsf{X})$ by $\mathfrak{T}$. More formally, we have

$$\mathcal{T}_{Point}(\mathsf{X}) = \mathfrak{T}(V(\mathsf{X})) \cap \mathbb{Z}^2 \tag{7}$$

In other words, the problem of digital rigid motion can be expressed as a problem of digitization of a continuous object. However, this continuous object $V(\mathsf{X})$ has a boundary consisting of pixel edges. In particular, such boundary is locally non-differentiable, and the approach proposed by Pavlidis for smooth-boundary object is then non-valid.

The issue of topology preservation in such non-differentiable case was investigated in [6]. This led to the definition of a notion of *digital regularity*[2].

Definition 3 (Digital regularity (from [6])) Let $\mathsf{X} \subset \mathbb{Z}^2$ be a digital object; we assume that X is well-composed. In addition, we assume that X has no singular points, *i.e.* for any $\mathsf{p} \in \mathsf{X}$ (resp. $\overline{\mathsf{X}}$), there exists a point $\mathsf{q} \in \mathsf{X}$ (resp. $\overline{\mathsf{X}}$) that is 4-adjacent to p. We say that X is *digitally regular* if for any couple $\{\mathsf{p}, \mathsf{q}\} \subset \mathsf{X}$ (resp. $\overline{\mathsf{X}}$) of 4-adjacent points, there exists a 2×2 square of points $\{\mathsf{x}, \mathsf{y}, \mathsf{z}, \mathsf{t}\} = \{\mathsf{x}, \mathsf{x} + (0, 1), \mathsf{x} + (1, 0), \mathsf{x} + (1, 1)\}$ such that $\{\mathsf{p}, \mathsf{q}\} \subset \{\mathsf{x}, \mathsf{y}, \mathsf{z}, \mathsf{t}\} \subseteq \mathsf{X}$ (resp. $\overline{\mathsf{X}}$).

This notion of digital regularity provides a sufficient condition for guaranteeing that a well-composed digital object X will not be topologically modified by any arbitrary rigid motion.

Proposition 3 ([6]) *If a well-composed object $\mathsf{X} \subset \mathbb{Z}^2$ is digitally regular, then it is topologically invariant under digitized rigid motions.*

However, despite this nice topological property, the notion of digital regularity does not tackle the issue of geometry alteration. Indeed, the rigid motion model, such as defined in Eqs. (5–7), acts on the object in a pointwise way. It is then unable to preserve the global coherence of the object boundary, thus leading to a "noisy" result. This is illustrated in Fig. 5.

[2] In [6] this notion was simply called *regularity*. We rename it as "digital" to avoid any ambiguity.

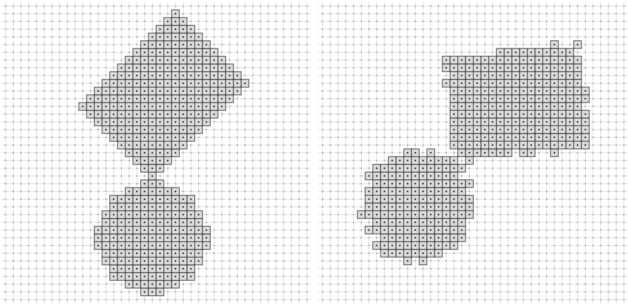

(a) (b)

Fig. 5 Geometry and topology alterations induced by digitized rigid motions. (a) A well-composed object, in grey. The object is non-digitally regular at the corners of the rectangle, and at the junction between the disk and the rectangle. (b) Digital rigid motion $\mathcal{T}_{Point}$ of (a). The digital boundary is more noisy than the initial object. In addition, we observe that the 4-connectivity has been lost at the junction between the disk and the circle, and at the opposite corner of the rectangle; this is a side effect of non-digital regularity in these areas.

2.5 Purpose and contributions

In this manuscript, our purpose is to find a way of performing rigid motions on digital objects, while preserving not only their topological properties, but also their geometric properties and more especially the general shape of their boundaries.

As discussed above, the main cause of boundary alteration when performing rigid motion is the fact that the transformation is computed pointwise; each point is transformed and then approximated independently from the others; see Eqs. (5–7).

In order to avoid this effect, we propose to carry out the rigid motion on a continuous model of the digital object X. However, by contrast with a trivial pixel model (see Sec. 2.4) that does not capture efficiently the boundary shape, we propose to consider a polygonal model of this boundary.

More precisely, our purpose is to define from $\mathsf{X} \subset \mathbb{Z}^2$ a polygon $P(\mathsf{X}) \subset \mathbb{R}^2$ that relevantly represents X. This means that the Gauss digitization of this polygon must be the initial object, *i.e.*

$$P(\mathsf{X}) \cap \mathbb{Z}^2 = \mathsf{X} \quad (8)$$

In addition, the boundary of $P(\mathsf{X})$ should fit reasonably the digital boundary of the digital object X.

Such polygon is a continuous object. It can then be processed by a continuous rigid motion, as described in Eq. (1). However, this continuous object is piecewise affine. Thus, it can also be handled in a discrete way, via its finite set of vertices.

Once transformed, the polygon has to be embedded back into $\mathbb{Z}^2$. This digitization step is algorithmically tractable, and can be made without approximation for polygons whose vertices have integer or rational coordinates.

The principal challenge of this process consists of working with polygons whose properties authorize the preservation of topology and geometry of the associated digital object. Then, we investigate sufficient conditions on such polygons —and more generally on continuous objects— for guaranteeing that their Gauss digitization will lead to coherent digital objects, fairly similar to the input objects. In other words, we aim at defining an analogue of the notion of Pavlidis' r-regularity, in the case of non-differentiable (including piecewise affine) objects. This notion will be called *quasi-r-regularity.*

In particular, two cases are studied. In Sec. 4, we consider the case of convex digital objects. In such scenario, the associated polygon is the convex hull of the object, and our purpose is then to retrieve a convex digital object as output. In Sec. 5, we consider the more general case of non-necessarily convex digital objects. In such scenario, various polygonization policies can be relevantly proposed.

It is important to notice that, in Secs. 4–5, we will only deal with simply connected objects, *i.e.* digital objects that are connected and without holes. The case of non-connected objects with holes may be handled without much difficulty from this simply connected case.

3 Quasi-r-regularity

We now introduce the notion of *quasi-r-regularity.* Intuitively, a quasi-r-regular object X of $\mathbb{R}^2$ presents sufficient conditions for guaranteeing that its connectedness will not be affected by a Gauss digitization process.

Let us first introduce some notations and few mathematical morphology notions. We note B_r (resp. C_r) a close disk (resp. a circle) of $\mathbb{R}^2$ of radius $r > 0$. We note $\oplus$, $\ominus$ and $\circ$ the classical operators of dilation, erosion and opening commonly used in mathematical morphology [12,18,19]. In particular, $\oplus$ is the Minkowski addition, $\ominus$ the associated subtraction, and $\circ$ the composition of both, that is $X \circ Y = X \ominus Y \oplus Y$.

Definition 4 (Quasi-r-regularity) Let $r > 0$. Let $X \subset \mathbb{R}^2$ be a finite, simply connected (*i.e.* connected and with no holes) object. If

- $X \ominus B_r$ is non-empty and connected;
- $\overline{X} \ominus B_r$ is connected;
- $X \subseteq X \ominus B_r \oplus C_{r\sqrt{2}}$; and
- $\overline{X} \subseteq \overline{X} \ominus B_r \oplus C_{r\sqrt{2}}$;

we say that X is *quasi-r-regular.*

Remark 1 This definition does not require specific properties on the boundary of X. In particular, it need not be differentiable.

Remark 2 If X is sufficiently large, and in particular if at least one disk $B_{1+\frac{\sqrt{2}}{2}}$ lies in X (*i.e.* $X \ominus B_{1+\frac{\sqrt{2}}{2}}$ is a non-empty set), the assertion "$X \subseteq X \ominus B_1 \oplus C_{\sqrt{2}}$" can be replaced by $X \subseteq X \ominus B_1 \oplus B_{\sqrt{2}}$; indeed, both are then equivalent in that case. Since $\overline{X}$ is non-finite, we can unconditionnally replace "$\overline{X} \subseteq \overline{X} \ominus B_1 \oplus C_{\sqrt{2}}$" by $\overline{X} \subseteq \overline{X} \ominus B_1 \oplus B_{\sqrt{2}}$.

Remark 3 In order to compare the two notions of quasi-r-regularity and of Pavlidis' r-regularity, we rewrite hereafter the definition of r-regularity of a finite, simply connected object $X \subset \mathbb{R}^2$: X is r-regular if:

- $X \ominus B_r$ is non-empty and connected;
- $\overline{X} \ominus B_r$ is connected;
- $X = X \ominus B_r \oplus B_r$; and
- $\overline{X} = \overline{X} \ominus B_r \oplus B_r$.

In particular we observe that the principal difference between both notions is the fact that the matching between X (resp. $\overline{X}$) and its opening need to be perfect in the case of r-regularity, while a "margin" is authorized in the case of quasi-r-regularity, thus allowing for non-smooth (for instance, non-differentiable, noisy...) boundary. Examples of quasi-1-regular and non-quasi-1-regular objects are given in Fig. 6. Perspectives related to this remark will be evoked in Sec. 7.

Proposition 4 *If X is quasi-1-regular, then $\mathsf{X} = X \cap \mathbb{Z}^2$ and $\overline{\mathsf{X}} = \overline{X} \cap \mathbb{Z}^2$ are both 4-connected. In particular, X is then well-composed.*

Proof We prove the 4-connectedness of X; the same reasonning holds for $\overline{\mathsf{X}}$. Let us first prove that $(X \circ B_1) \cap \mathbb{Z}^2$ is 4-connected. Let p and q be two distinct points of $(X \circ B_1) \cap \mathbb{Z}^2$. Let B_1^{p} and B_1^{q} be two disks of radius 1, included in $X \circ B_1$ and such that $\mathsf{p} \in B_1^{\mathsf{p}}$ and $\mathsf{q} \in B_1^{\mathsf{q}}$. (Such disks exist, from the very definition of opening.) Let b_{p} and b_{q} be the centers of B_1^{p} and B_1^{q}, respectively. We have $b_{\mathsf{p}}, b_{\mathsf{q}} \in X \ominus B_1$, from the very definition of erosion. Since $X \ominus B_1$ is connected in $\mathbb{R}^2$; there exists a continuous path Π from b_{p} to b_{q} in $X \ominus B_1$. Note that for any a disk B_1, we always have $B_1 \cap \mathbb{Z}^2$ non-empty and 4-connected; in particular it contains at least two points of $\mathbb{Z}^2$. For a value $\varepsilon > 0$ sufficiently small, two disks B_1 and B_1' with centres distant of ε are such that $B_1 \cap B_1' \cap \mathbb{Z}^2 \neq \emptyset$. As a consequence, the union $\bigcup_{b \in \Pi} B_1(b) \cap \mathbb{Z}^2$ (with $B_1(b)$ the disk of center b) is a 4-connected set of $\mathbb{Z}^2$. In addition, we have $\mathsf{p}, \mathsf{q} \in \bigcup_{b \in \Pi} B_1(b) \cap \mathbb{Z}^2$. Then, p and q are 4-connected in $(X \circ B_1) \cap \mathbb{Z}^2$, and it follows that $(X \circ B_1) \cap \mathbb{Z}^2$ is a 4-connected set. Let us now prove that any point $\mathsf{r} \in X \setminus (X \circ B_1)$ is 4-adjacent to a point of $(X \circ B_1) \cap \mathbb{Z}^2$. Let us consider such point r. We have $\mathsf{r} \in X \subseteq X \ominus B_1 \oplus C_{\sqrt{2}}$. Then, from the very definition of dilation, there exists $b \in X \ominus B_1$ such that b is the centre of a circle $C_{\sqrt{2}}(b)$ of radius $\sqrt{2}$, and r is a point of this circle. In particular, the distance between b and r is $\sqrt{2}$. As b is a point of $X \ominus B_1$, it is also the centre of a disk $B_1(b)$ of radius 1 included in $X \circ B_1$. Let us consider the circle $C_1(\mathsf{r})$ of radius 1 and centre r. This circle $C_1(\mathsf{r})$ intersects $B_1(b)$, and this intersection is a circular segment of radius 1 and angle $\pi/4$, included in $X \circ B_1$. Then, this segment necessarily contains a point $\mathsf{t} \in \mathbb{Z}^2$, that lies in $(X \circ B_1) \cap \mathbb{Z}^2$. The points r and t are 4-adjacent. It follows that $X \cap \mathbb{Z}^2$ is 4-connected. $\square$

This notion of quasi-r-regularity will be used in the next two sections for guaranteeing the preservation of topological properties digital objects during rigid motions, via their (continuous) polygonal representation.

4 Rigid motions of digitally convex objects

In this section, we first deal with a specific case of digital objects, namely the convex ones. For rigid motion purpose, we build a continuous polygon corresponding to the convex hull of the input digital object. Then, we move this continuous polygon, and we finally redigitize it for retrieving the final transformed digital object. We show that, by this process, the digital convexity is preserved if the convex hull is quasi-1-regular.

4.1 Digital convexity

In the Euclidean space $\mathbb{R}^2$, an object X is said to be convex if, for any pair of points $\mathrm{x}, \mathrm{y} \in \mathrm{X}$, the line segment joining x and y

$$[\mathrm{x}, \mathrm{y}] = \{\lambda \mathrm{x} + (1-\lambda)\mathrm{y} \in \mathbb{R}^2 \mid 0 \leq \lambda \leq 1\} \tag{9}$$

is included in X. However, this intuitive continuous notion cannot be directly transposed to digital objects of $\mathbb{Z}^2$. Indeed, given a digital object X in $\mathbb{Z}^2$, for $\mathsf{p}, \mathsf{q} \in \mathsf{X}$ we generally have $[\mathsf{p}, \mathsf{q}] \not\subset \mathbb{Z}^2$.

In order to tackle this problem, various extensions of the notion of convexity have been proposed for $\mathbb{Z}^2$. We can cite, for instance: MP-convexity [20] which is a straightforward extension of the continuous notion; S-convexity [21] which uses convex objects in $\mathbb{R}^2$ to determine the convexity of objects in $\mathbb{Z}^2$; H-convexity [22] which is a geometrical version of S-convexity, using the convex-hull of digital objects; and D-convexity [23] which is based on the notion of digital line.

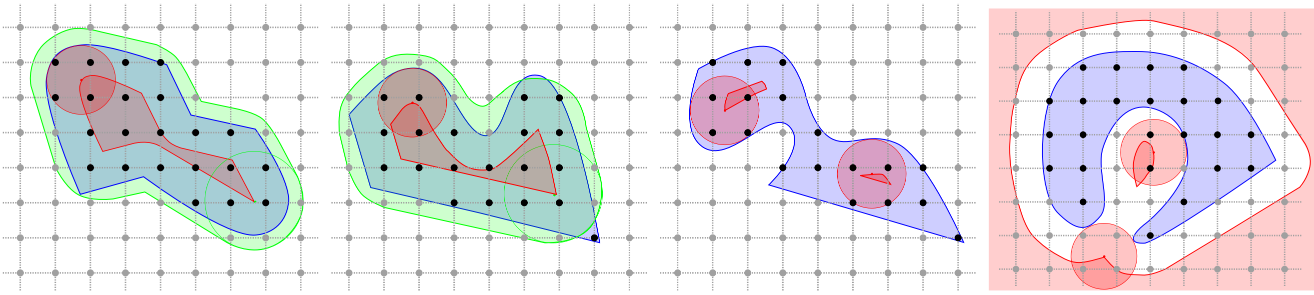

(a) Quasi-1-regular (b) Non-quasi-1-regular (c) Non-quasi-1-regular (d) Non-quasi-1-regular

Fig. 6 Examples of quasi-1-regular (a) and non-quasi-1-regular (b,c,d) objects X: (b) $X \nsubseteq X \ominus B_1 \oplus C_{\sqrt{2}}$; (c) $X \ominus B_1$ is not connected; (d) $\overline{X} \ominus B_1$ is not connected. The objects $X \subset \mathbb{R}^2$ are in blue, the balls B_1 are in red, the circles $C_{\sqrt{2}}$ are in green, the erosions $X \ominus B_1$ are in red and $X \ominus B_1 \oplus C_{\sqrt{2}}$ are in green.

In the case of 4-adjacency modeling of digital objects, MP- and H-convexities have been proved equivalent [22, Theorem 5]. Similar results under the assumption of 8-adjacency can be found in [24], via the chord property, which relate the MP-, H- and D-convexities. Under the condition that X has no isolated point (*i.e.* no point adjacent to one other point within X), it was then proved that X is H-convex iff it is S-convex [22, Theorem 4]. A more complete description on various notions of digital convexity can be found in [25, Chapter 9].

In this section, the notion of H-convexity was chosen. This is motivated, on the one hand, by its compliance with the other kinds of convexities in the case of 4-connected (and, a fortiori, well-composed) digital objects. On the other hand, the notion of H-convexity relies on the explicit definition of the convex hull of the digital object. Such polygonal object provides us with a continuous model that can be involved in the continuous part of our rigid motion algorithmic process.

We recall hereafter the definition of the convex hull of a digital object $\mathsf{X} \subset \mathbb{Z}^2$, denoted by $\mathcal{Conv}(\mathsf{X})$. Then, we provide the formal definition of H-convexity.

$$\mathcal{Conv}(\mathsf{X}) = \left\{ \mathrm{x} = \sum_{i=1}^{|\mathsf{X}|} \lambda_i \mathsf{p}_i \in \mathbb{R}^2 \;\middle|\; \sum_{i=1}^{|\mathsf{X}|} \lambda_i = 1 \wedge \forall i \in [\![1, |\mathsf{X}|]\!] (\lambda_i \geq 0 \wedge \mathsf{p}_i \in \mathsf{X}) \right\} \tag{10}$$

Definition 5 (H-convexity [22]) A digital object $\mathsf{X} \subset \mathbb{Z}^2$ is H-convex if

$$\mathsf{X} = \mathcal{Conv}(\mathsf{X}) \cap \mathbb{Z}^2 \tag{11}$$

i.e. if X is equal to the (re)digitization of its continuous polygonal convex hull.

It is important to notice that, similarly to continuous convexity, H-convexity remains stable by intersection, as stated by the following property.

Property 1 Let X and Y be two digital objects in $\mathbb{Z}^2$. If X and Y are H-convex, then $\mathsf{X} \cap \mathsf{Y}$ is H-convex.

4.2 Polygonization of H-convex digital objects

The first step of the algorithmic process for computing the rigid motion of a H-convex digital object X consists of computing its polygonal convex hull.

If X contains at least three non-colinear points, then its convex hull $\mathcal{Conv}(\mathsf{X})$ is a non-trivial convex polygon whose vertices are some points of X. As these vertices are grid points of $\mathbb{Z}^2$, the polygon $\mathcal{Conv}(\mathsf{X})$ is defined as the intersection of closed half-planes with integer coefficients

$$\mathcal{Conv}(\mathsf{X}) = \bigcap_{\mathrm{H} \in \mathcal{R}(\mathsf{X})} \mathrm{H} \tag{12}$$

where $\mathcal{R}(\mathsf{X})$ is the set of all closed half-planes that include X. This set is infinite. However, a finite subset of $\mathcal{R}(\mathsf{X})$ is indeed sufficient for defining $\mathcal{Conv}(\mathsf{X})$. Each closed half-plane H of this subset is defined as

$$\mathrm{H} = \{(x, y) \in \mathbb{R}^2 \mid ax + by + c \leq 0\} \tag{13}$$

with $a, b, c \in \mathbb{Z}$ and $\gcd(a, b) = 1$. Note that the integer coefficients of H are uniquely obtained by a pair of consecutive vertices of $\mathcal{Conv}(\mathsf{X})$, denoted by $\mathsf{u}, \mathsf{v} \in \mathbb{Z}^2$, which are in the clockwise order, such that

$$(a, b) = \frac{1}{\gcd(w_x, w_y)}(-w_y, w_x) \tag{14}$$

$$c = (a, b) \cdot \mathsf{u} \tag{15}$$

where $(w_x, w_y) = \mathsf{v} - \mathsf{u} \in \mathbb{Z}^2$.

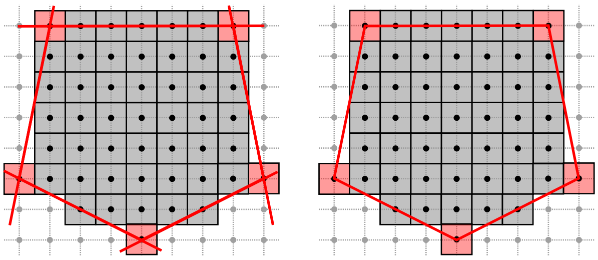

Fig. 7 A digital H-convex object X of $\mathbb{Z}^2$ (black dots and grey pixels). (a) The half-plane representation of X, depicted by the 5 red support lines. The red points/pixels are those required to define these closed half-spaces. (b) The convex hull $\mathcal{C}onv(\mathsf{X})$ in $\mathbb{R}^2$, defined as the polygon whose vertices are these red points.

Many algorithms can be used to compute the convex hull of a digital object. In [26], a linear time algorithm determines whether a given polyomino is convex and, in that case, it returns its convex-hull. This method relies on the incremental digital straight line recognition algorithm [27], and uses the geometrical properties of leaning points of maximal discrete straight line segments on the contour. The algorithm scans the contour curve and decomposes it into discrete segments whose extremities must be leaning points. The tangential cover of the curve [28] can be used to obtain this decomposition. Alternatively, an approach presented in [29] uses tools of combinatorics on words to study contour words: the linear Lyndon factorization algorithm [30] and the Christoffel words. A linear time algorithm decides convexity of polyominoes and can also compute the convex hull of a digital object (it is presented as a discrete version of the classical Melkman algorithm [31]).

The half-planes can then be deduced from the consecutive vertices of the computed convex hull, from Eqs. (13–15). An example of convex hull and half-plane modeling of a H-convex digital object is illustrated in Fig. 7.

4.3 Convexity-preserving rigid motion

In order to perform rigid motions without any numerical approximation, a reasonable approach consists of considering only rigid motions with rational parameters. Doing so, only exact computations with integers can be involved. This does not constitute an applicative restriction, due to the density of "relevant" rational values within the rotation and translation parameter space.

Thus, we assume hereafter that all the parameters of a rigid motion $\mathfrak{T}$ are rational (see Eq. (1)). More precisely, on the one hand, the rotation matrix R is defined as $\frac{1}{r}\begin{pmatrix} p & -q \\ q & p \end{pmatrix}$ where $p, q, r \in \mathbb{Z}$ constitute a Pythagorean triple, *i.e.* $p^2+q^2 = r^2, r \neq 0$. On the other hand, the translation vector is defined as $(t_x, t_y)^t \in \mathbb{Q}^2$. This assumption is fair, as we can always find rational parameter values sufficiently close to any real values [32] for defining such a Pythagorean triple.

A half-plane H, as defined in Eq. (13), is transformed by such (rational) rigid motion $\mathfrak{T}$ as follows

$$\mathfrak{T}(\mathrm{H}) = \{(x, y) \in \mathbb{R}^2 \mid \alpha x + \beta y + \gamma \leq 0\} \tag{16}$$

where $\alpha, \beta, \gamma \in \mathbb{Q}$ are given by $(\alpha\ \beta)^t = R(a\ b)^t$ and $\gamma = c + \alpha t_x + \beta t_y$. This leads to a rational half-plane, which can be easily rewritten as an integer half-plane in the form of Eq. (13).

Since a H-convex digital object X is represented by a finite set of digital half-planes, we can define the rigid motion $\mathcal{T}_{\mathcal{C}onv}$ of X on $\mathbb{Z}^2$ via its continuous polygonal convex hull as follows

$$\mathcal{T}_{\mathcal{C}onv}(\mathsf{X}) = \mathfrak{T}(\mathcal{C}onv(\mathsf{X})) \cap \mathbb{Z}^2 = \mathfrak{T}\Bigg(\bigcap_{\mathrm{H} \in \mathcal{R}(\mathsf{X})} \mathrm{H}\Bigg) \cap \mathbb{Z}^2 \tag{17}$$

where $\mathcal{R}(\mathsf{X})$ is the set of all half-planes including X. This constitutes an alternative to the standard point-wise rigid motion defined in Eq. (5).

But, we have

$$\begin{aligned} \mathfrak{T}\Bigg(\bigcap_{\mathrm{H} \in \mathcal{R}(\mathsf{X})} \mathrm{H}\Bigg) \cap \mathbb{Z}^2 &= \Bigg(\bigcap_{\mathrm{H} \in \mathcal{R}(\mathsf{X})} \mathfrak{T}(\mathrm{H})\Bigg) \cap \mathbb{Z}^2 \\ &= \bigcap_{\mathrm{H} \in \mathcal{R}(\mathsf{X})} (\mathfrak{T}(\mathrm{H}) \cap \mathbb{Z}^2) \end{aligned} \tag{18}$$

The digitization of any continuous half-space of $\mathbb{R}^2$ is H-convex. Then, from Eqs. (17–18), $\mathcal{T}_{\mathcal{C}onv}(\mathsf{X})$ is expressed as the intersection of a finite number of H-convex digital objects. The following proposition is then a corollary of Property 1.

Proposition 5 *Let X be a digital object of $\mathbb{Z}^2$. Let $\mathcal{T}_{\mathcal{C}onv}$ be the polygon-based rigid motion induced by a rigid motion $\mathfrak{T}$ with rational parameters. If X is H-convex, then $\mathcal{T}_{\mathcal{C}onv}(\mathsf{X})$ is H-convex.*

Remark 4 The polygon corresponding to the convex hull of $\mathcal{T}_{\mathcal{C}onv}(\mathsf{X})$ is not equal, in general, to the transformed continuous polygon corresponding to the convex hull of X. However, we have the following inclusion relation

$$\mathcal{C}onv(\mathcal{T}_{\mathcal{C}onv}(\mathsf{X})) \subseteq \mathfrak{T}(\mathcal{C}onv(\mathsf{X})) \tag{19}$$

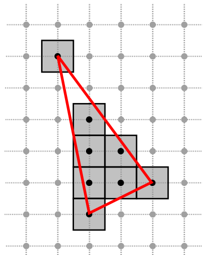

Fig. 8 A digital object X that is H-convex, but not connected. This is due, here, to the acute angle at the highest vertex of the convex hull $\mathcal{C}onv(\mathsf{X})$ that allows the induced polygon to "pass between" two 4-adjacent points of the background of X.

First, it means that the cardinality of $\mathcal{T}_{\mathcal{C}onv}(\mathsf{X})$ is lower (often strictly) than that of X. In other words, $\mathcal{T}_{\mathcal{C}onv}$ is a decreasing operator with respect to the cardinality of the input digital object. A straightforward consequence is that $\mathcal{T}_{\mathcal{C}onv}$ is not bijective, in general. Second, it means that the polygons of the two convex hulls of the input and output digital objects may be distinct, with respect to their number and size of edges, and angles at vertices. However, the convexity of the objects is preserved, which was the fundamental property to satisfy. These facts are experimentally observed in Sec. 6.

4.4 Rigid motions and topological aspects of convexity

In the previous subsections, we proposed an algorithmic scheme for performing rigid motions on H-convex digital objects, while preserving their H-convexity. In $\mathbb{R}^2$, the continuous definition of convexity intrinsically implies connectedness. By contrast, in $\mathbb{Z}^2$ the notion of H-convexity (such as various other notions of digital convexity) does not always offer guarantees of connectedness, *e.g.* with respect to 4- and 8-adjacencies.

In order to illustrate that fact, let us consider the example of Fig. 8. The digital object X, composed of 8 points/pixels, is H-convex. Indeed, its convex hull contains only digital points that belong to X. However, X is not connected (neither with 4- nor 8-adjacencies). Such phenomenon is mainly caused by angular and/or metric factors: whenever an angle of the convex hull polygon is too acute, and/or when an edge is too short, such disconnections may happen.

Then, in addition to providing geometry guarantees of convexity —via the H-convexity of digital objects— when performing rigid transformations of a digital object, it is desirable to also provide topology guarantees, and more precisely connectedness guarantees.

To reach that goal, we use the notion of *quasi-r-regularity* introduced in Sec. 3. This additional notion will provide us with sufficient conditions for ensuring that a digital H-convex object will remain not only H-convex but also connected after any rigid motion.

In particular, the next proposition is a direct corollary of Propositions 4 and 5.

Proposition 6 *Let $\mathsf{X} \subset \mathbb{Z}^2$ be a H-convex digital object. If $\mathcal{C}onv(\mathsf{X})$ is quasi-1-regular, then $\mathcal{T}_{\mathcal{C}onv}(\mathsf{X})$ is H-convex, 4-connected and well-composed.*

Remark 5 If $\mathcal{C}onv(\mathsf{X})$ is quasi-1-regular, then the initial object X is also 4-connected and well-composed.

5 Rigid motions of general digital objects

In this section, we now deal with rigid motions of digital objects without convexity hypothesis.

5.1 Polygonization of a digital object

There exist various methods for polygonizing a digital object. In the field of digital geometry, numerous approaches used the contour curves extracted from the digital objects; each method computes a polygonal representation of the digital object with particular properties. In [33,34], invertible methods allow to compute Euclidean polygons whose redigitization is equal to the original discrete boundary. These methods use the Vittone's algorithm [35] in the preimage space for straight line recognition. In [36–39] the arithmetical recognition algorithm [27] is used to decompose a discrete contour and deduce a polygonal representation. These methods rely on the tangential cover of the contour [28], composed of the sequence of its maximal discrete straight segments. It was proved in [36] that all polygonal representations of the contour can be deduced from its tangential cover, leading to a linear algorithm which computes the polygon with minimal integral summed squared error. In [37–39], the goal was different. It consisted of determining a reversible polygon that faithfully represents the convex and concave parts of the boundary of a digital object. The polygonization method proposed in [40,41] also exploits the idea of maximal straight segment primitives. It allows to identify the characteristic points on a contour, called dominant points, and to build a polygon representing the given contour. Another technique presented in [42] is the curve decomposition. It uses the analytical primitives, called digital level layers, to decompose a given contour and to obtain an analytical representation. Another algorithm is proposed in [43] to compute the polygonal simplification of a curve such that the Fréchet distance between the simplified polygon and the original curve is lower than a given error.

It should be mentioned that, for a given digital object, different results can be obtained from these various polygonization techniques. In other words, the polygonal representation of a digital object is not unique. However, the crucial property to be satisfied is that the polygon $P(\mathsf{X})$ computed for a digital object X has to be coherent with respect to redigitization, *i.e.* $P(\mathsf{X}) \cap \mathbb{Z}^2 = \mathsf{X}$. A second important property, in our framework of discrete geometry and exact calculus, is that the vertices of $P(\mathsf{X})$ have integer or rational coordinates. Some other relevant, but sometimes antagonistic, properties are discussed in Sec. 5.3.

Our chosen polygonization policy will be described in the experimental section (Sec. 6). In particular, it guarantees the two above properties and polygon vertices have integer coordinates.

5.2 Rigid motion of a polygon

As $P(\mathsf{X})$ may be non-convex, we cannot use half-planes representation, as it was done in Sec. 4.2 for convex polygons. Here, we use a standard vertex representation, by modeling the polygon via the sequence of successive vertices of its boundary.

Note that the vertices of $P(\mathsf{X})$ are integer points, and those of $\mathfrak{T}(P(\mathsf{X}))$ are rational points, since the rigid motion $\mathfrak{T}$ is given by a rational matrix and a rational translation vector (see Sec. 4.3).

Then, for each vertex of the polygon $P(\mathsf{X})$, we simply apply the rigid motion $\mathfrak{T}$ (see Eq. (1)) and preserve the order of the vertex sequence.

5.3 Discretization of polygons and geometry / topology preservation

Once the polygon $\mathfrak{T}(P(\mathsf{X}))$ has been computed, the resulting object, noted $\mathcal{T}_{\mathcal{P}oly}(\mathsf{X})$ can be deduced. Similarly to the case of H-convex digital objects (Eq. (17)), this is done by embedding $\mathfrak{T}(P(\mathsf{X}))$ in $\mathbb{Z}^2$ via a Gauss digitization

$$\mathcal{T}_{\mathcal{P}oly}(\mathsf{X}) = \mathfrak{T}(P(\mathsf{X})) \cap \mathbb{Z}^2 \tag{20}$$

Various ways exist for carrying out this digitization in an exact way. For instance, it is possible to decompose $\mathfrak{T}(P(\mathsf{X}))$ into a partition of triangles whose vertices are (rational coordinate) vertices of the boundary of $\mathfrak{T}(P(\mathsf{X}))$. Each such triangle being defined as a convex region modeled by three half-planes with rational parameters, the points of $\mathbb{Z}^2$ contained herein can be determined without numerical error.

In order to ensure the connectedness preservation of X, we require, as for the H-convex case, that the digital object be quasi-1-regular.

Proposition 7 *Let $\mathsf{X} \subset \mathbb{Z}^2$ be a digital object. Let $P(\mathsf{X}) \subset \mathbb{R}^2$ be a polygon such that $P(\mathsf{X}) \cap \mathbb{Z}^2 = \mathsf{X}$. If $P(\mathsf{X})$ is quasi-1-regular, then $\mathcal{T}_{\mathcal{P}oly}(\mathsf{X})$ is 4-connected and well-composed.*

Remark 6 If $P(\mathsf{X})$ is quasi-1-regular, then the initial object X is also 4-connected and well-composed. Beyond these topological guarantees, the quasi-1-regularity also provides geometry guarantees. Indeed, the presence of discrete points within each disk B_1 located either in the opening $P(\mathsf{X}) \circ B_1$ or $\overline{P(\mathsf{X})} \circ B_1$, combined to the fact that the "oulier" discrete points are located at a distance not greater than $\sqrt{2} - 1 < 0,5$ (*i.e.* lower than half a pixel length) from these openings, avoids noisy effects that may be caused by standard pointwise rigid motions $\mathcal{T}_{Point}$ (see Sec. 2.4).

As stated above, the polygon $P(\mathsf{X})$ can be defined by following various policies. Then, there exist many (actually an infinite number of) polygons whose redigitization leads to X. In particular, it may happen that $P(\mathsf{X})$ is *not* quasi-1-regular while X and $\mathcal{T}_{\mathcal{P}oly}(\mathsf{X})$ are indeed 4-connected and well-composed.

This statement emphasizes the importance of choosing wisely a polygonization policy. In this context, various properties may be relevantly targeted.

A first property is related to the preservation of area. Indeed, due to the digitization procedure of the polygon, carried out by a regular sampling with respect to $\mathbb{Z}^2$, it may be useful that $P(\mathsf{X})$ has an area in $\mathbb{R}^2$ equal to the cardinal $|\mathsf{X}|$. This is justified by the fact that each pixel (*i.e.* Voronoi cell) of a point of $\mathbb{Z}^2$ as an area of 1 in $\mathbb{R}^2$.

A second property is related to the positioning of $P(\mathsf{X})$ with respect to X. More precisely, it may be relevant that the barycentre of both $P(\mathsf{X})$ and X be the same. Otherwise, the shift between both may statistically induce a translation bias in the rigid motion result.

A third property is to "fit at best" the polygon $P(\mathsf{X})$ with a differentiable boundary continuous object, *i.e.* to minimize the size of the regions located inside $P(\mathsf{X})$ (resp. $\overline{P(\mathsf{X})}$) but outside of $P(\mathsf{X}) \circ B_1$ (resp. $\overline{P(\mathsf{X})} \circ B_1$). There is no unique and good answer to this question. Indeed, the choice actually depends, on the one hand, on the hypotheses about the semantics of the digital object (is it a digital model of an underlying differentiable object or a non-differentiable one? is it a true discrete set, not related to a continuous object? *etc.*). On the other hand, making a polygonal object minimize the areas lying outside its opening (and the opening of

	 #Points=316				
	$\theta = \frac{\pi}{5}$	$\theta = \frac{2\pi}{5}$	$\theta = \frac{3\pi}{5}$	$\theta = \frac{4\pi}{5}$	$\theta = \pi$
$\mathcal{T}_{Point}(\mathsf{X})$	 #Points=315	 #Points=311	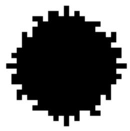 #Points=319	 #Points=320	 #Points=318
$\mathcal{T}_{\mathcal{C}onv}(\mathsf{X})$	 #Points=282	 #Points=258	 #Points=215	 #Points=174	 #Points=148
$\mathcal{T}_{Poly}(\mathsf{X})$	 #Points=282	 #Points=288	 #Points=291	 #Points=288	 #Points=316

Table 1 Experiments on geometry and topology preservation on a disk of radius 10, for rotations of angle θ (the rotation centre is the centre of the disk). See Sec. 6.1.

its complement) generally requires to consider angles at vertices that tend toward π, and edges whose length tends toward 0. Such polygons may present a higher space cost (and then, time cost, when processed). In addition, the relevance of their shape may be questionable, since "short" continuous edges may be weakly related to the digital line segments intrinsically modeling a digital object X.

6 Experiments

In this section, we present some experimental results obtained with the proposed method on different digital objects. The comparison, in terms of topology and geometry, between three models of rigid motion on convex objects is first discussed. Then, numerical experiments are performed on non-convex objects to evaluate, more generally, the effect of rigid motions on boundaries of digital objects.

It should be mentioned that the digital objects used in these experiments have their associated polygons being quasi-1-regular. For an efficient computation, we use the discrete version of the Melkman algorithm [31] to compute the convex hull of H-convex objects. This algorithm has a linear time complexity with respect to the number of digital points. Concerning the polygonization, we apply the method of dominant point detection proposed in [40,41] with adaptation in order to obtain a result satisfying the property $P(\mathsf{X}) \cap \mathbb{Z}^2 = \mathsf{X}$. More precisely, from the polygon P of dominant points, we run through the contour points of X between two consecutive dominant points and select those that enclose all contour points being outside of P. It is shown in [27] that dominant point detection algorithm can be achieved with a linear time complexity with respect to the number of contour points. Furthermore, the algorithm involves exact computation with integers and the obtained polygon has integer vertices.

6.1 Topology and geometry preservation of convex digital objects under rotations

We carried out experiments on two H-convex digital objects, namely a disk of radius 10 and a square of size 20×20, in order to provide a first assessment of the performance of rigid motions using three transformation models: pointwise ($\mathcal{T}_{Point}$, see Sec. 2.3); based on

#Points=400

	$\theta = \frac{\pi}{5}$	$\theta = \frac{2\pi}{5}$	$\theta = \frac{3\pi}{5}$	$\theta = \frac{4\pi}{5}$	$\theta = \pi$
$\mathcal{T}_{Point}(\mathsf{X})$	 #Points=400	 #Points=399	 #Points=403	 #Points=401	 #Points=401
$\mathcal{T}_{Conv}(\mathsf{X})$	 #Points=320	 #Points=308	 #Points=268	 #Points=236	 #Points=200
$\mathcal{T}_{Poly}(\mathsf{X})$	 #Points=320	 #Points=328	 #Points=328	 #Points=320	 #Points=400

Table 2 Experiments on geometry and topology preservation on a square of size 20×20, for rotations of angle θ (the rotation centre is the barycentre of the square). See Sec. 6.1.

convex hull ($\mathcal{T}_{Conv}$, see Sec. 4.3); and based on polygons ($\mathcal{T}_{Poly}$, see Sec. 5.2).

The first of these experiments was conducted under a sequence of successive rotations, to evaluate the topology and geometry alterations accumulated in the transformed images. The experiment is as follows: a rotation is applied on the input image; then the transformed image is used as input for the next rotation, and so on. Tables 1 and 2 provide the visual results of rotated images by the three transformation models on the disk and the square, respectively.

We observe that the rigid motions by $\mathcal{T}_{Point}$ alter the boundary of the objects. They do not only modify their topology but also their geometry. Indeed, the initial disk and square objects are well-composed and H-convex; however the transformed objects are not. By contrast, the rigid motions by $\mathcal{T}_{Conv}$ allow us to preserve both topology and geometry properties. However, as mentioned in Sec. 4.3, $\mathcal{T}_{Conv}$ is a decreasing operator with respect to the cardinality of the input object (see Remark 4). The rigid motions by $\mathcal{T}_{Poly}$ avoid this effect since $\mathcal{T}_{Poly}$ is based on a polygon that fits the size of the digital object in a better way than the convex hull.

6.2 Quantitative evaluation of transformations on convex digital objects

Now, we aim to quantify experimentally the accuracy and stability of the three models of rigid motions on convex digital objects. More precisely, we observe two measures: (i) the area (*i.e.* the number of digital points) of the transformed objects; and (ii) the perimeter of the polygons extracted from these transformed objects.

Two series of experiments are performed: the first with rotations for angles θ varying from 0 to 2π; the second with rigid motions randomly generated.

Figs. 9 and 10 report some quantitative comparisons between rotations by $\mathcal{T}_{Point}$, $\mathcal{T}_{Conv}$ and $\mathcal{T}_{Poly}$ on the input images given in Tables 1 and 2. We can see that $\mathcal{T}_{Poly}$ preserves better the periodicity under rotations compared to $\mathcal{T}_{Point}$ and $\mathcal{T}_{Conv}$.

Figs. 11 and 12 show results under rigid motions. These rigid motions are generated randomly with rotation angles $\theta \in [0, 2\pi)$ and translations $a, b \in [0, 1)$. Since $\mathcal{T}_{Point}$ may disturb the digital boundary, the perimeter tends to change at each iteration. As $\mathcal{T}_{Conv}$ is a decreasing operator, the area of the transformed objects is reduced at each iteration. By contrast, $\mathcal{T}_{Poly}$

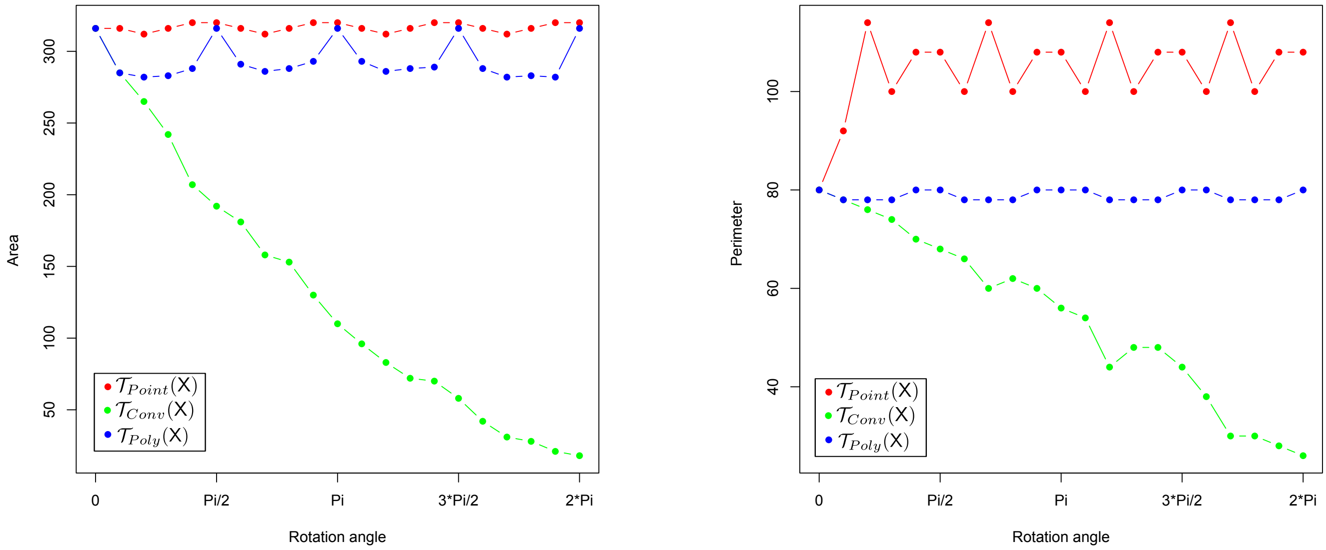

Fig. 9 Area (left) and perimeter (right) variations induced by successive rotations for the disk of radius 10 of Table 1. See Sec. 6.2.

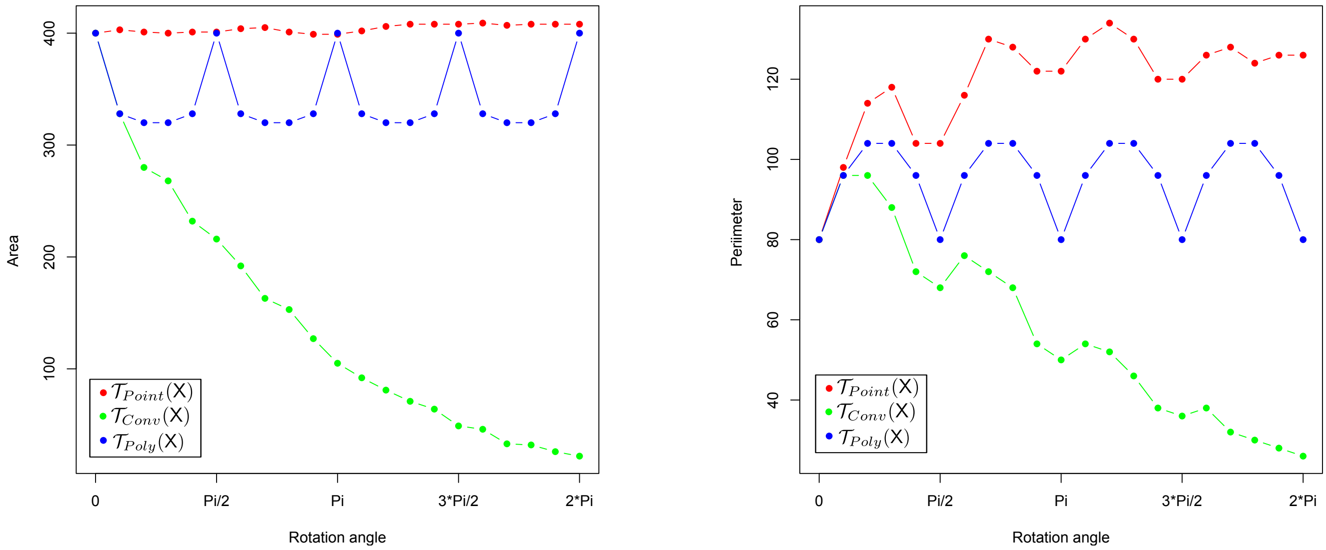

Fig. 10 Area (left) and perimeter (right) variations induced by successive rotations for the square of size 20×20 of Table 2. See Sec. 6.2.

better preserves both the area and perimeter of the transformed objects.

6.3 Quantitative evaluation of transformations on non-convex digital objects

In these last experiments, we perform rigid motions on non-convex objects (see Fig. 13). Again, we evaluate the proposed transformation model $\mathcal{T}_{Poly}$ with respect to the following measures: (i) the area (*i.e.* the number of digital points in the transformed object); and (ii) the perimeter of the polygons extracted from these transformed objects.

The results are shown in Fig. 14, for successive rigid motions $\mathcal{T}_{Poly}$ generated randomly with rotation angles $\theta \in [0, 2\pi)$ and translations $a, b \in [0, 1)$. We can observe that $\mathcal{T}_{Poly}$ as a stable behaviour with respect to the considered geometry measures.

7 Conclusion

In this article, we proposed an algorithmic process for performing rigid motions on digital objects, *i.e.* finite

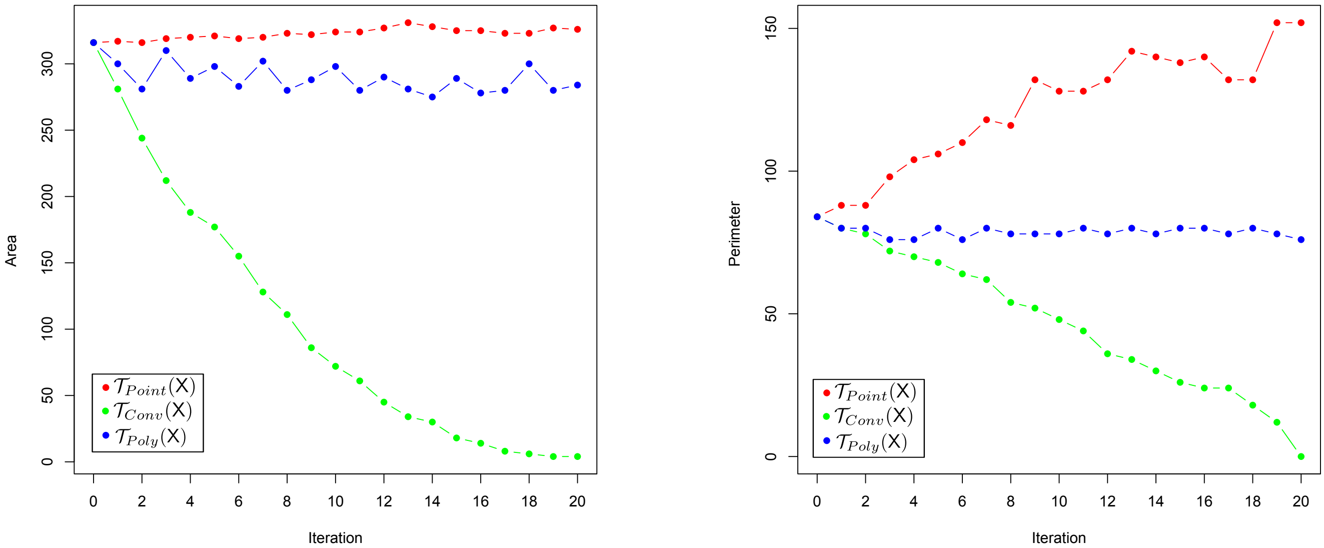

Fig. 11 Area (left) and perimeter (right) variations induced by successive rigid motions for the disk of radius 10 of Table 1. See Sec. 6.2.

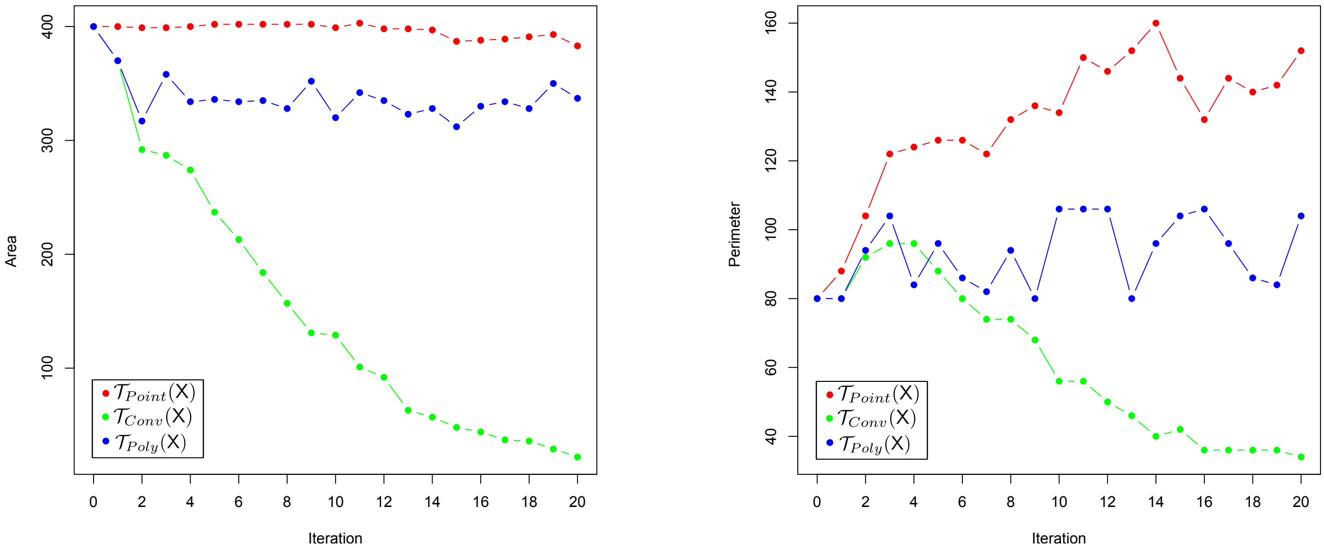

Fig. 12 Area (left) and perimeter (right) variations induced by successive rigid motions for the square of size 20×20 of Table 2. See Sec. 6.2.

subsets of $\mathbb{Z}^2$, while preserving their global shape. This shape preservation was expressed in terms of geometry, but also in terms of topology, since the object should not be erroneously disconnected due to the discrete structure of $\mathbb{Z}^2$. In order to tackle these issues, our contributions were twofold. From a methodological point of view, we proposed to consider an intermediate continuous model of the digital object, namely a polygonal model. Such polygon is continuous and can then be processed by standard continuous transformations; it also remains discrete, and can then be processed without numerical error. From a theoretical point of view, we proposed a new notion of quasi-r-regularity that provides sufficient conditions for guaranteeing topological preservation when digitizing a continuous object. This notion of quasi-r-regularity was indeed required to correctly handle the mandatory redigitization step induced by the use of an intermediate continuous polygonal model.

This work opens the way to various perspectives. First we will investigate how this rigid motion scheme can be extended to the 3D case, *i.e.* to digital objects defined in $\mathbb{Z}^3$. In addition, we will describe how to consider not only simply connected objects, but more generally arbitrary-topology objects (this is tractable in $\mathbb{Z}^2$, but less simple in $\mathbb{Z}^3$). Second, from a practical point of

(a) X_1 (b) X_2 (c) X_3

Fig. 13 Non-convex digital objects used as input for the experiments of Sec. 6.3.

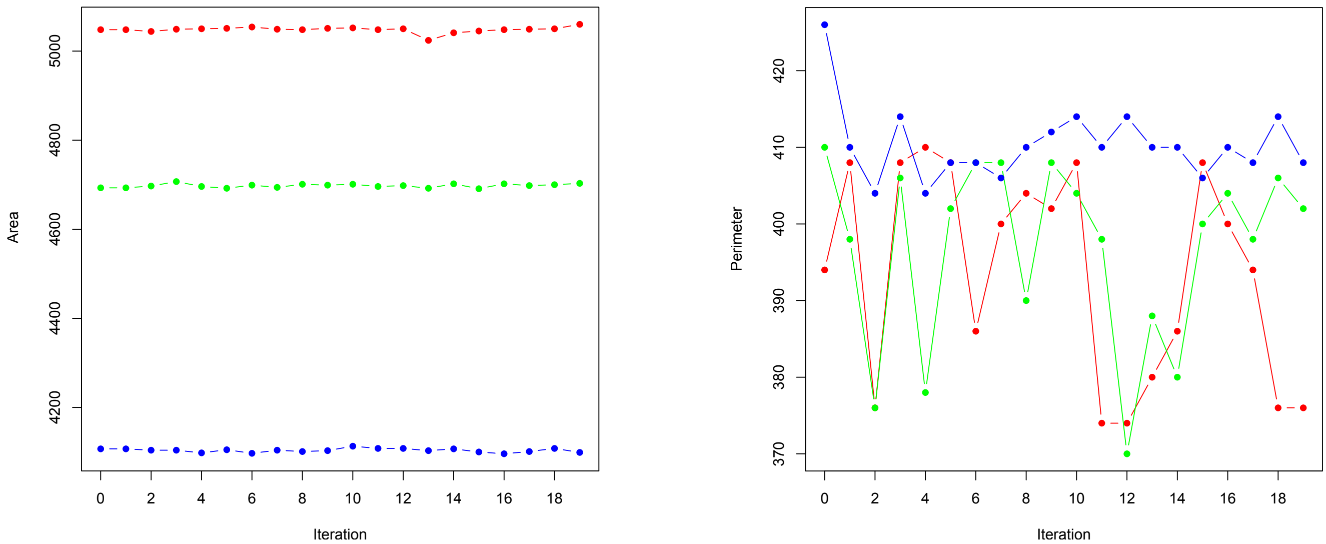

Fig. 14 Area (left) and perimeter (right) evolution of the three digital objects X_1, X_2 and X_3 (see Fig. 13), under successive rigid motions $\mathcal{T}_{Poly}$. See Sec. 6.3.

view, we will investigate the relevance of different polygonization approaches, in order to identfy those that are the best fitted to the proposed transformation approach. We will also investigate digital objects that correspond to limit cases, just beyond the domain of validity of quasi-1-regularity; indeed, some of these objects (often thin, or small-sized) may preserve some topological properties, although not being quasi-1-regular. Third, we will explore more deeply the notions of regularity. In particular, we will aim at proposing a notion that may encompass both the notions of Pavlidis' r-regularity and of quasi-r-regularity. Such notion could allow us to better understand —and handle— the intrinsic mechanisms of topology-preserving digitization, in various regular grids, adjacency models and space dimensions.

References

1. B. Zitová, J. Flusser, Image registration methods: A survey, Image and Vision Computing 21 (11) (2003) 977–1000.
2. S. Faisan, N. Passat, V. Noblet, R. Chabrier, C. Meyer, Topology-preserving warping of binary images according to one-to-one mappings, IEEE Transactions on Image Processing 20 (8) (2011) 2135–2145.
3. P. Ngo, Y. Kenmochi, N. Passat, H. Talbot, Combinatorial structure of rigid transformations in 2D digital images, Computer Vision and Image Understanding 117 (4) (2013) 393–408.
4. K. Pluta, P. Romon, Y. Kenmochi, N. Passat, Bijective digitized rigid motions on subsets of the plane, Journal of Mathematical Imaging and Vision 59 (1) (2017) 84–105.
5. P. Ngo, Y. Kenmochi, N. Passat, H. Talbot, Topology-preserving conditions for 2D digital images under rigid transformations, Journal of Mathematical Imaging and Vision 49 (2) (2014) 418–433.
6. P. Ngo, N. Passat, Y. Kenmochi, H. Talbot, Topology-preserving rigid transformation of 2D digital images,

IEEE Transactions on Image Processing 23 (2) (2014) 885–897.
7. T. Pavlidis, Algorithms for Graphics and Image Processing, Berlin: Springer, and Rockville: Computer Science Press, 1982.
8. P. Ngo, Y. Kenmochi, I. Debled-Rennesson, N. Passat, Convexity-preserving rigid motions of 2D digital objects, in: Discrete Geometry for Computer Imagery, Vol. 1568, 1999, pp. 31–40.
9. R. Klette, A. Rosenfeld, Digital Geometry: Geometric Methods for Digital Picture Analysis, Elsevier, Amsterdam, Boston, 2004.
10. L. Mazo, N. Passat, M. Couprie, C. Ronse, Digital imaging: A unified topological framework, Journal of Mathematical Imaging and Vision 44 (1) (2012) 19–37.
11. T. Yung Kong, A. Rosenfeld, Digital topology: Introduction and survey, Computer Vision, Graphics, and Image Processing 48 (3) (1989) 357–393.
12. J. Serra, Image Analysis and Mathematical Morphology, Academic Press, Inc., Orlando, FL, USA, 1983.
13. L.J. Latecki, C. Conrad, A. Gross, Preserving topology by a digitization process, Journal of Mathematical Imaging and Vision 8 (2) (1998) 131–159.
14. P. Stelldinger, U. Köthe, Towards a general sampling theory for shape preservation, Image and Vision Computing 23 (2) (2005) 237–248.
15. C.R.F. Maunder, Algebraic Topology, Dover, New York, 1996.
16. A. Rosenfeld, Digital topology, American Mathematical Monthly, 86 (8) (1979), 621–630.
17. L.J. Latecki, U. Eckhardt, A. Rosenfeld, Well-composed sets, Computer Vision and Image Understanding 61 (1) (1995), 70–83.
18. H.J.A.M. Heijmans, C. Ronse, The algebraic basis of mathematical morphology. I Dilations and erosions, CVGIP: Image Understanding 50 (3) (1990), 245–295.
19. C. Ronse, H.J.A.M. Heijmans, The algebraic basis of mathematical morphology: II. Openings and closings, CVGIP: Image Understanding 54 (1) (1991), 74–97.
20. M. Minsky, S. Papert, Perceptrons: An Introduction to Computational Geometry, MIT Press, Reading, MA, 1969.
21. J. Sklansky, Recognition of convex blobs, Pattern Recognition 2 (1) (1970) 3–10.
22. C.E. Kim, On the cellular convexity of complexes, IEEE Transactions on Pattern Analysis and Machine Intelligence 3 (6) (1981) 617–625.
23. C.E. Kim, A. Rosenfeld, Digital straight lines and convexity of digital regions, IEEE Transactions on Pattern Analysis and Machine Intelligence 4 (2) (1982) 149–153.
24. U. Eckhardt, Digital lines and digital convexity, in: Digital and Image Geometry: Advanced Lectures, 2001, pp. 209–228.
25. G. Cristescu, L. Lupsa, Non-Connected Convexities and Applications, Dordrecht: Kluwer Academic Publishers, 2002.
26. I. Debled-Rennesson, J.-L. Rémy, J. Rouyer-Degli, Detection of the discrete convexity of polyominoes, Discrete Applied Mathematics 125 (1) (2003) 115–133.
27. I. Debled-Rennesson, J. Reveillès, A linear algorithm for segmentation of digital curves, International Journal of Pattern Recognition and Artificial Intelligence 9 (4) (1995) 635–662.
28. F. Feschet, L. Tougne, Optimal time computation of the tangent of a discrete curve: Application to the curvature, in: Discrete Geometry for Computer Imagery, Vol. 1568, 1999, pp. 31–40.
29. S. Brlek, J. Lachaud, X. Provençal, C. Reutenauer, Lyndon + Christoffel = digitally convex, Pattern Recognition 42 (10) (2009) 2239–2246.
30. J. Duval, Factorizing words over an ordered alphabet, Journal of Algorithms 4 (4) (1983) 363–381.
31. A.A. Melkman, On-line construction of the convex hull of a simple polyline, Information Processing Letters 25 (1) (1987) 11–12.
32. W.S. Anglin, Using Pythagorean triangles to approximate angles, American Mathematical Monthly 95 (6) (1988) 540–541.
33. I. Sivignon, R. Breton, F. Dupont, E. Andres, Discrete analytical curve reconstruction without patches, Image and Vision Computing 23 (2) (2005) 191–202.
34. M. Dexet, D. Coeurjolly, E. Andres, Invertible polygonalization of 3D planar digital curves and application to volume data reconstruction, in: International Symposium on Visual Computing, Vol. 4292, 2006, pp. 514–523.
35. J. Vittone, J.-M. Chassery, Recognition of digital naive planes and polyhedrization, in: Discrete Geometry for Computer Imagery, Vol. 1953, 2000, pp. 296–307.
36. F. Feschet, L. Tougne, On the min DSS problem of closed discrete curves, Discrete Applied Mathematics 151 (1–3) (2005) 138–153.
37. H. Dörksen-Reiter, I. Debled-Rennesson, Convex and concave parts of digital curves, in: Geometric Properties for Incomplete Data, 2006, pp. 145–159.
38. H. Dörksen-Reiter, I. Debled-Rennesson, A linear algorithm for polygonal representations of digital sets, in: International Workshop on Combinatorial Image Analysis, Vol. 4040, 2006, pp. 307–319.
39. T. Roussillon, I. Sivignon, Faithful polygonal representation of the convex and concave parts of a digital curve, Pattern Recognition 44 (10–11) (2011) 2693–2700.
40. T.P. Nguyen, I. Debled-Rennesson, A discrete geometry approach for dominant point detection, Pattern Recognition 44 (1) (2011) 32–44.
41. P. Ngo, H. Nasser, I. Debled-Rennesson, Efficient dominant point detection based on discrete curve structure, in: International Workshop on Combinatorial Image Analysis, Vol. 9448, 2015, pp. 143–156.
42. Y. Gérard, L. Provot, F. Feschet, Introduction to digital level layers, in: Discrete Geometry for Computer Imagery, Vol. 6607, 2011, pp. 83–94.
43. I. Sivignon, A near-linear time guaranteed algorithm for digital curve simplification under the Fréchet distance, in: Discrete Geometry for Computer Imagery, Vol. 6607, 2011, pp. 333–345.
44. T.P. Nguyen, I. Debled-Rennesson, Curvature estimation in noisy curves, in: Computer Analysis of Images and Patterns, Vol. 4673, 2007, pp. 474–481.